Nat. Hazards Earth Syst. Sci. Discuss., doi:10.5194/nhess-2016-381, 2016
Manuscript under review for journal Nat. Hazards Earth Syst. Sci.
Published: 9 December 2016

Natural Hazards and Earth System Sciences
Discussions
Open Access

Combination of empirically-based and physically-based methods to assess shallow slides susceptibility at the basin scale

Sérgio C. Oliveira[1], José L. Zêzere[1], Sara Lajas[1],Raquel Melo[1]

[1]Centre for Geographical Studies, IGOT (Institute of Geography and Spatial Planning), Universidade de Lisboa, Edifício IGOT, Rua Branca Edmée Marques, 1600-276 Lisboa, Portugal

Correspondence to: Sérgio C. Oliveira (cruzdeoliveira@campus.ul.pt)

Abstract. Approaches used to assess shallow slides susceptibility at the basin scale are conceptually different depending on the use of empirically-based or physically-based methods. The former are sustained by the assumption that the same causes are more likely to produce the same effects, whereas the latter are based on the comparison between forces which tend to promote movement along the slope and the opposing forces that promote resistance to movement. Within this general framework, this work tests two hypotheses: (i) although conceptually and methodological distinct, the statistic and deterministic methods generate similar shallow slides susceptibility results regarding the model's predictive capacity and spatial agreement; and (ii) the combination of shallow slides susceptibility maps obtained with empirically-based and physically-based methods, for the same study area, generate a more reliable susceptibility model for shallow slides occurrence. These hypotheses were tested in a small test site (13.9 km^2) located north of Lisbon (Portugal), using a empirically-based method (the Information Value method) and a physically-based method (the Infinite Slope method). The landslide susceptibility maps produced with the statistic and deterministic methods were combined into a new landslide susceptibility map. The latter was based on a set of integration rules defined by the cross-tabulation of the susceptibility classes of both maps and analysis of the corresponding contingency tables. The results demonstrate a higher predictive capacity of the new shallow slides susceptibility map, which combines the independent results obtained with empirically-based and physically-based models. Moreover the combination of the two models allowed the identification of areas where the results of the Information Value and the Infinite Slope methods are contradictory. Thus, these areas were classified as uncertain and deserve additional investigation at a more detailed scale.

Keywords: Shallow slides, susceptibility, Information Value, Infinite Slope, Factor of Safety, models combination.

1 Introduction

The evaluation of landslide susceptibility have been made worldwide supported by three fundamental principles (Varnes et al., 1984; Carrara et al., 1991; Hutchinson, 1995; Guzzetti, 2005): (i) landslide can be recognized, classified and mapped; (ii) the conditions that cause instability (predisposing factors) can be identified, registered and used to build predictive models; (iii) the occurrence of landslide can be spatially inferred. Within this conceptual scheme, it is assumed that future landslides are more likely to occur in areas where geologic and geomorphologic conditions are similar to those that originate the slope instability in the past (Guzzetti et al., 1999). This conceptual scheme has been extended to different methods of landslide susceptibility assessment, regardless of their nature (Varnes et al., 1984; Hutchinson, 1995; Aleotti and Chowdhury, 1999; Carrara et al., 1999; Fell et al., 2008b). This is nonetheless surprising since the conceptual model is perfectly applied to any empirically-based method used to assess landslide susceptibility, but the same is not true for the physically-based methods. Indeed, the latter methods are based on physical laws and soil mechanics principles, being the slope understood as a system where shear stress and shear strength are continually in opposition. That is, unlike what happens with statistical methods, deterministic methods are applicable not accounting the landslide inventory, which, however, is still essential to validate the obtained landslide susceptibility results.

The comparison between different methods to assess landslide susceptibility is not a new research topic when performed exclusively between different empirically-based statistical methods (Gorsevski et al., 2003; Süzen and Doyuran, 2004; Brenning, 2005; Davis et al., 2006; Lee et al., 2007; Felicísimo et al., 2013; Bui et al., 2016) or between different physically-based methods (Zizioli et al., 2013; Formetta et al., 2014; Pradham and Kim, 2015; Teixeira et al., 2015). Regarding the comparison of the predictive capacity between empirically-based and physical-based methods, a few number of works exist (Crosta et al., 2006; Carrara et al., 2008; Frattini et al., 2008; Yilmaz and Keskin, 2009; Cervi et al., 2010; Goetz et al., 2011) and from those only a limited number of studies have combined the results obtained with empirically-based and physically-based approaches (Chang and Chiang, 2009; Goetz et al., 2011). According to Zizioli et al. (2013) the different methods used to assess shallow slides susceptibility are not mutually exclusive. The latter authors pointed out that the use of different strategies to assess landslide susceptibility and the comparison of their predictive capacity can help to: (i) enhance the quality and reliability of each method; (ii) highlight and identify the most important factors affecting the slope instability system; (iii) neglect less influential aspects to simplify the models; and (iv) select the most appropriate methodology to achieve a specified goal.

In this study we aim to verify two hypotheses: (i) although conceptually and methodologically distinct, the statistic and deterministic methods generate similar results for shallow landslides susceptibility regarding the model's predictive capacity and spatial agreement; and (ii) the combination of the shallow landslides susceptibility maps obtained with empirically-based and physically-based methods, for the same study area, generate a more reliable susceptibility map for shallow slides occurrence.

2 Study area

The study area comprises the two small catchments of Monfalim and Louriceira (13.9 km^2), which are located 25 km NNW of Lisbon, Portugal (Fig. 1). The elevation ranges from 442 m at the West to 134 m in the northeast sector of the study area, near the confluence of both Monfalim and Louriceira rivers with the Grande da Pipa River (GPR), which is affluent of the Tagus River.

The lithological units are mainly constituted by sedimentary rocks dated from the Kimmeridgian to the Lower Thitonian (Upper Jurassic). Alluvium deposits of Holocene age and a complex of dikes and volcanic masses are also present, both covering only 1.1 % of the study area. The detailed lithological units map for the study area shown in Fig. 1 was constructed based on existing official geological maps (Zbyszewski and Assunção, 1965; INETI, 2005), but also on interpretation of aerial photographs and validation of lithological units limits through field work. Therefore, it was possible to identify eight lithological units enumerated here according the age criteria, being progressive older: (i) alluvium; (ii) Arranhó formation (limestones and marls); (iii) Sobral formation (sandstones and limestones); (iv) Sobral formation (mudstones and marls); (v) Amaral formation (limestones); (vi) Amaral formation (marls); (vii) Abadia formation (mudstones and marls). The lithological unit (viii) is constituted by dykes and volcanic masses (basalt, teschenite, dolerite and weathered rocks).

The study area suffered since the Miocene a wide curvature angle tectonic rebound (Zbyszewski and Assunção, 1965) and the layers dip typically to SE/SW. This structural setting together with the alternation of soft rocks such as marls, clays and mudstones with more resistant rocks as the limestones allowed the development of cuesta-like landforms resulting from differential erosional processes (Ferreira, 1984; Ferreira et al., 1987; Zêzere, 1991). Therefore, in the study area gentle reverse slopes are found over the lithologic units of Sobral and Arranhó formations, whereas abrupt cutting slopes are present along the Amaral limestones lithological unit that outcrops over the erosive depression mainly excavated in the Abadia marls and mudstones formation (Ferreira, 1984). The slopes within the study area are typically moderate: 78.1 % of the total area is within the slope range from 5º to 20º. The gentle slopes (0º – 5º) represent only 12.9 % and the steepest slopes (> 20º) occur only in 9 % of the study area.

Landslides in the study area have been triggered by rainfall (Zêzere et al., 1999, 2005, 2015; Zêzere and Rodrigues, 2002; Oliveira, 2012). The climate is Mediterranean and the Mean Annual Precipitation (MAP) is 730 mm (at São Julião do Tojal gauge located 20 km south from the study area) (Zêzere et al., 2015). Shallow slides have been triggered mainly by intense short duration rainfall episodes, typically not exceeding 1 to 15 days (Zêzere and Trigo, 2011; Zêzere et al., 2015). These rainfall events generate the accretion of pore water pressure and the reduction of the soil shear strength, including the loss of cohesion on fine sediments, which promotes the failure along the superficial soil formations or along the contact between the soil and the impermeable bedrock (Trigo et al., 2005).

3 Methods and data

The methodological procedures for assessing shallow slides susceptibility based on the application and combination of empirically-based and physically-based approaches are summarized in Fig. 2. Two commonly used methods were chosen: the bivariate statistical Information Value (IV) method (Yin and Yan, 1988) and the Infinite Slope method (IS) (Sharma, 2002) sustained on the calculation of the Factor of Safety (FS). Both methods are in line with the experts panel recommendations to assess landslide susceptibility (Cascini, 2008; Fell et al., 2008a, 2008b; Corominas et al., 2014) and have been applied successfully in similar geological and geomorphological context in the region north of Lisbon (Zêzere, 2002; Pimenta, 2011; Guillard and Zêzere, 2012; Oliveira et al., 2015). For shallow slides susceptibility modelling, the dependent variables (shallow slides modelling and validation groups), the independent dataset of variables used as predisposing factors, and the maps representing geotechnical and hydrological parameters were rasterized using a pixel of 5 x 5 m.

3.1 Landslide inventory

The landslide inventory is used twofold in this study: (i) to establish the statistical relationships between shallow slides and the data-set of environmental factors assumed as shallow slides predisposing factors in the empirically-based approach; and (ii) to validate the shallow slides susceptibility models obtained with both empirically-based and physically-based models. The landslide inventory of the study area (Fig.1) includes 111 shallow slides (translational slides and rotational slides with high curvature angle of the slip surface) that were classified according to Cruden and Varnes (1996) classification. The depth of the slip surface is typically less than 1.5 m. The shallow slides inventory was extracted from (Oliveira, 2012) and was based on interpretation of aerial photographs (1983, 1989) and orthophotomaps (2003, 2004, 2007), as well as on extensive field work made during the period 2006-2010.

The inventory of shallow slides was further subjected to a partition based on a temporal criterion (Fig.1, Table 1). The landslide training group includes the shallow slides that occurred until the end of 1983 (51 cases, 0.027 km^2, and 0.19 % of the study area). The landslide validation group includes all landslides occurred after 1983 until the end of 2010 (60 cases, 0.03 km^2, 0.22 % of the study area. The training group was used to weight classes of shallow slides predisposing factors in the statistical model using the IV method, and was also used to calibrate the shear strength parameters (cohesion and friction angle) of the lithological formations in the IS model. The validation group was used for the independent validation of both empirically-based and physically-based shallow slides susceptibility models.

3.2 Empirically-based approach to assess landslide susceptibility

3.2.1. The Information Value method

The Information Value (IV) (Yin and Yan, 1988) was used to compute the susceptibility score for each class of each variable considered as landslide predisposing factor based on the log normalization of the ratio between the conditional probability to find a shallow slide in a certain class of a predisposing factor and the a priori probability to find a shallow slide in the study area, following the Eq. (1).

$$\mathrm{Lxi} = \log \frac{\mathrm{Si/Ni}}{\mathrm{S/N}} \ , \tag{1}$$

where: Lxi is the Information Value of class xi belonging to an independent variable (predisposing factor); Si is the number of pixels with shallow slides belonging to the training group and the presence of the variable class xi; Ni is the number of pixels with variable class Xi; S is the total number pixels with shallow slides belonging to the training group; and N is the total number of pixels of the study area. Due to the logarithmic normalization li is not calculated when Si = 0. In those cases li was determined as the lowest value considering the complete data set of predisposing factors. Final IV scores (Lxi) for each terrain unit (j) was obtained using Eq. (2).

$$\mathrm{Lj} = \sum_{\mathrm{i}=1}^{\mathrm{m}} \mathrm{Xij\ Ii} \ , \qquad (2)$$

where: m is the total number of variable classes; and Xij is either 0 if the variable class is not present in the pixel j, or 1 if the variable class is present.

3.2.2 Landslide predisposing factors

In this work, we selected as independent variables seven landslide predisposing factors (Fig. 3, Fig. 1 and Table 4 for the description of classes) that have been used with success in previous studies in the region north of Lisbon (e.g., (Oliveira et al., 2015): lithology, slope angle, slope aspect, slope curvature, topographic position index (TPI), slope over area ratio and land use.

The lithologic map includes 8 classes that were already described (cf. Sect. 2. Study area). The Land use map was obtained from the official map representing the land use observed in 1990. Although does not match to the current land use in the study area, this is the one that best fits the time span of shallow landslides included in the present landslide inventory and the temporal land use frame closer to the age of landslides training group. The remaining variables (slope, aspect, curvature, topographic position index and slope over area ratio) were derived from a Digital Elevation Model based on elevation data interpolated from a topographic contours map (equidistance 10 m). For the curvature map, a DEM generalization based on a 50 m pixel size grid was considered to calculate the profile of the slopes, which prove to best fit the morphology of slopes in the study area (Oliveira et al., 2015). The Topographic Position Index (TPI) was calculated based on the Facet Corridor Designer tool for ArcGIS (Jenness et al., 2011). As the index is heavily dependent on the scale (Piacentini et al., 2015) an interactively neighbourhood radius of 25 meters for index calculation proved to be the most appropriate to the work reference scale. The Slope Over Area Ratio (SOAR) was used to express the importance of the topography in hydrological processes by the relation between the slope and the contribution area (Sørensen et al., 2006), which allow to infer the areas prone to surface saturation (Fonseca, 2005). The calculation of the SOAR was made using the TauDEM 5.2 (Terrain Analysis Using Digital Elevation Models) tool and considering the algorithm D8 (O'Callagham and Mark, 1984) to minimize the dispersion of accumulation flow.

3.3 Physically-based approach to assess landslide susceptibility

3.3.1 The Infinite Slope method (IS)

The most popular formulations of the Infinite Slope method consider a subsurface flow/water table level parallel to the topographic surface, introducing that way, the saturated soil thickness factor. In this context, the development of a steady-state hydrological model in static conditions can be related to the ratio between the thickness of saturated soil and the thickness of the potentially unstable soil as provided in the formulation of SHALSTAB model (Dietrich and Montegomery, 1998). The FS for each terrain unit (pixel) was thus calculated based on the Infinite Slope method, incorporating a soil thickness model and an hydrologic model for the study area, following Eq. (3) (Sharma, 2002):

$$\mathrm{FS} = \frac{c' + h * \cos^2\beta[(1-m)\Upsilon_m + m\,\Upsilon_{sub}] * \tan\phi'}{h * \sin\beta * \cos\beta[(1-m)\Upsilon_m + m\,\Upsilon_{sat})}, \qquad (3)$$

Where: c′ is the effective cohesion (kN/m²); h is the potentially unstable soil depth; β is the slope of the terrain unit; m is the equation component of the hydrological model, considered as the ratio between the saturated soil depth and the potentially unstable soil depth; ϕ′ is the internal friction angle (°); γ_m is the specific soil weight (kN/m³); γ_{sat} is the saturated soil weight (kN/m³) and γ_{sub} is the submerged soil weight (kN/m³). The FS values can be interpreted in two ways. In the more restrict sense it is assumed that all terrain units with FS values ≤ 1 are unstable. A more broad interpretation turns possible to compare FS results with results obtained from the empirically-based approach; this is, to consider that each terrain unit within a study area could be tier according FS values being more susceptible the terrain unit as lower the FS value.

The development of the IS model was supported by the following parameters: (i) topographical variables (slope and catchment area), (ii) soil thickness, (iii) hydrologic parameters (hydraulic conductivity, soil transmissivity and daily rainfall threshold), (iv) geotechnical parameters (natural, saturated and submerged specific soil weights; cohesion; and internal friction angle). Most geotechnical parameters were deduced from references with regional validity that were summarized by (Pimenta, 2011).

3.3.2 Soil thickness model

The depth of the soil potentially unstable is a critical parameter that strongly influences the stability of slopes. The soil depth model for the study area was obtained following Eq. (4), as proposed by (Catani et al., 2010):

$$h = -K_c . C . \eta . \Psi^{-1}, \qquad (4)$$

Where: h is the soil thickness, K_c is a constant calibration parameter, C is an index based on the slope profile curvature, η is the relative soil depth dependent on the topographic position; ψ^{-1} is the critical slope angle associated to landslide occurrence. The three parameters C, η and ψ-1 were expressed by linear normalization into a dimensionless index with values ranging between 0 and 1. The constant K_c was estimated independently for each lithological unit based on trial and error estimation to fit as much as possible the soil thickness values obtained by Eq. 4 to the soil thickness values measured in 110 sampling field points. These sampling field measurements were spatial distributed in order to guarantee a reasonable number of soil thickness measurements in each lithological unit but also along different geomorphological units (interfluve areas, slopes, valley floors), although dependent of the existence of slope cuts where the soil depth was measured. To accept the K_c constant calibration for any lithological unit, the differences between the maximum estimated soil thickness and the maximum soil thickness measured in the field should not exceed 1 m. Table 2 summarizes the K_c constant calibration values obtained for each lithological unit in the study area. Soil profiles were not found in LU1, LU3 and LU8 during the field work. In the case of LU 3, we adopted a K_c value equal to the one estimated for the other lithologic unit belonging to the Sobral formation (LU 4, $K_c = 3.6$). In the case of alluvium (LU1) and complex of dikes and masses (LU9) we adopted a K_c = 2.9, which is the arithmetic mean of all K_c values obtained for lithological units where it was possible to measure soil thickness during field sampling. Fig. 4 shows the final soil thickness map of the study area.

3.3.3 Hydrological model

The adopted hydrological model is based on the equation provided by SHALSTAB (Dietrich and Montegomery, 1998), supported by (O' Loughlin, 1986) model. According to Sharma (2002), the hydrologic model corresponds to the ratio between the thickness of saturated soil and the thickness of the potentially unstable soil, according to Eq. (5).

$$\frac{h}{z} = \frac{Q}{T} * \frac{a}{b * \mathrm{Sin}\beta}, \tag{5}$$

Where: h/z is the ratio between the thickness of the saturated soil above the impermeable layer and the thickness of the potentially unstable soil; Q is the effective precipitation (m/day); T is the transmissivity of the soil (m^2/day); a is the upstream contribution area (m2); b is the cell length (m); and β is the slope gradient (°). The increase of the hydrologic ratio (Q/T) indicates that soil saturation will be faster and more extensive. The topographic ratio (a/(b * Sinβ)) describes the topography effect on runoff (Dietrich and Montegomery, 1998; Montgomery et al., 1998). The transmissivity of the soil was estimated using Eq. (6) (Lencastre and Franco, 2006):

$$T = k + z, \tag{6}$$

Where: T is the soil transmissivity (m^2/day); k is the saturated hydraulic conductivity (m/day); and z is the soil thickness (m). As the hydraulic conductivity based on field measurements was not available for the study area, this parameter was estimated for the different soil types existing in the study area based on the work developed by (Rawls et al., 1982), which

Nat. Hazards Earth Syst. Sci. Discuss., doi:10.5194/nhess-2016-381, 2016
Manuscript under review for journal Nat. Hazards Earth Syst. Sci.
Published: 9 December 2016

summarized the typical hydraulic conductivities for different soil types starting from the respective textural properties. The national digital soil map at 1: 25,000 scale was used to extract the clay, silt + sand, and coarse sand fractions for the different soils types present in the study area. The soil taxonomy of the US Department of Agriculture was used to distinguish between soil types, through the Soil Texture Triangle Bulk Density. Rocky outcrops and urban areas were assigned with a -1 value, thus corresponding to 0 (absence of water) in the hydrological model. The castanozems soils were also assigned with a -1 value because the typical pedological stage of castanozem soils within the study area is a stony soil phase. At final, 55 types of soils were identified, in addition to social areas and rocky outcrops.

The effective precipitation was estimated based on the Eq. (7) proposed by Trigo et al. (2005) which defines the rainfall threshold for triggering translational and rotational landslides in the region north of Lisbon, which includes the study area.

$$\mathrm{Cr} = 7.4\mathrm{D} + 107 \, , \tag{7}$$

Where: Cr is the rainfall threshold that is associated to landslides occurrence (mm), and D is the number of consecutive rainfall days.

Most landslide events occur in the study area during the Winter season, so we assume that effect of evapotranspiration can be neglected and the effective precipitation can be assumed equal to total precipitation, namely for short rainfall periods. Using Eq. (7) we obtained a critical daily rainfall for failure of 114.4 mm (0.1144 m). The rainfall concentrated in a single day is a feasible scenario for triggering of shallow landslide events, as it happened in the Lisbon Region in 1967 and 1983 (Zêzere et al., 2005, 2015).

The hydraulic conductivity was estimated based on the critical precipitation for failure and the soil texture. In the study area k ranges from 5.05 m/day in the luvisols with dominantly sandy texture to 0.0144 m/day in vertisols with dominantly clayey texture. The computed transmissivity ranges between 0 and 13.45 m^2/day (Fig. 5A). The final hydrological model is shown in Fig. 5B.

3.3.4 Geotechnical parameters of superficial soils

All geotechnical parameters mentioned in this section, related to soil weight (Ym, Ysat Ysub) cohesion (c') and friction angle (ϕ'), were based on literature and were defined for the superficial soils above the bedrock within each lithological unit. The specific (Y_m), saturated (Y_{sat}) and submerged (Y_{sub}) soil weights values were provided by (Pimenta, 2011) and are summarized in Table 3.

The strength parameters of the lithological units obtained in laboratory with direct shear tests (Pimenta, 2011) proved to be too high to explain the observed slope instability. Therefore, the optimal combinations of cohesion and effective internal friction angle values for each lithological unit were defined iteratively through back analysis. Different combinations of cohesion and effective internal friction angles were tested in the Infinite Slope method and validated with the landslide training group (landslide area) using as reference the maximum and minimum friction angles suggested by (Geotechdata, 2013). Critical pairs of cohesion and internal friction angle were selected for each lithological unit by combining two criteria: (i) the susceptibility class with FS ≤ 1 must include at least 50 % of landslide area of the landslide training group located on the lithological unit; and (ii) the susceptibility class with FS ≤ 1 must have the highest effective ratio. The effective ratio of a susceptibility class (Chung and Fabbri, 2003) is expressed, by the ratio between the percentage of landslide area predicted in the class and the percentage of the class area in the study area. For LU2 and LU5 it was not possible to comply with the criterion (i), but the corresponding critical pair cohesion / internal friction angle were selected respecting criterion (ii). In addition, strength parameters of LU1 and LU8 were not possible to estimate with this method, due to the absence of landslides in these lithological units. In these cases, the cohesion and effective internal friction angle were derived directly from (Pimenta, 2011), which gathered information from technical reports, geotechnical laboratory tests and standard values reported in the literature (Baptista, 2004; Cernica, 1995; Fernandes, 1994; Jeremias, 2000; Vallejo et al., 2002). Table 3 summarizes the geotechnical parameters of the lithological units used for implementing the physically-based model.

3.4. Validation, comparison and combination of shallow slides susceptibility models

The validation of susceptibility maps produced by empirically-based and physically-based models was made independently using the landslide validation group. ROC (Receiver Operating Characteristic) curves were computed and the corresponding Area Under the Curve (AUC) was calculated. Additionally, the landslide susceptibility maps were classified and the effective ratio of each class was estimated. Both empirically-based and physically-based susceptibility maps were classified considering the same fraction of study area in each equivalent landslide susceptibility class. First, the IS map was classified into 5 classes based on the Factor of Safety values (≤ 1, 1 to 1.25; 1.25 to 1.5, 1.5 to 2, and > 2), which have correspondence, respectively, on the following descriptive classification of susceptibility (Very high; High; Moderate, Low; and Very low). In a second step, the IV map was classified into 5 classes (Very high; High; Moderate, Low; Very low), ensuring that equivalent susceptibility classes cover the same fraction of the study area in both maps. The evaluation of the spatial agreement between landslide susceptibility maps based on empirically-based and physically-based approaches was made using the Rank Difference Tool included in ArcSDM (Sawatzky et al., 2008).

Lastly, empirically-based and physically-based susceptibility maps were combined into a final shallow slides susceptibility map based on the intersection of the susceptibility classes in a contingency table using the Map Comparison Kit tool (e.g., Visser and Nijs, 2006), on a cell by cell comparison and Kappa statistics.

4 Results and discussion

4.1 Empirically-based landslide susceptibility assessment

The Information Value scores calculated for each class of predisposing factors based on the landslide training group are summarized in Table 4, and the corresponding shallow slides susceptibility map is shown in Fig. 6. The spatial distribution

Nat. Hazards Earth Syst. Sci. Discuss., doi:10.5194/nhess-2016-381, 2016
Manuscript under review for journal Nat. Hazards Earth Syst. Sci.
Published: 9 December 2016

of susceptibility shows a clear contrast between north/northeast sectors of the study area in which the susceptibility is predominantly classified as low to very low, whereas in the centre/south part of the study area the susceptibility to shallow slides is typically higher. This contrast is mainly justified by the lithological differentiation. In fact, in the northern part of the study area the LU7 (Abadia formation: marls and clays) and LU5 (Amaral formation: limestones) are found, which apparently have a low predisposition to shallow slide occurrence (Table 4). By opposition, lithological units more prone to slope instability (LU2 - Arranhó formation: limestones and marls; and LU3 - Sobral formation: sandstones and limestones) outcrop in the centre and south part of the study area. In addition, the slope angle tends to be higher in the latter part of the study area, thus contributing for the higher landslide susceptibility.

The ROC curve of the landslide susceptibility model is shown in Fig. 7. The model predictive capacity is reasonable/good, as expressed by the AUC ROC of 0.75.

4.2 Physically based landslide susceptibility assessment

The shallow slides susceptibility map computed with the IS method is shown in Fig. 8A. The susceptibility class with FS $\leq$1 (Very high susceptibility) covers 17.9 % of the total study area and validates 53.4 % of the shallow slides belonging to the landslide validation group, which explains the higher effective ratio (2.98) of this susceptibility class (Table 5). By comparison with the IV susceptibility map, it is evident the increment of area classified with very high/high susceptibility in the north sector of the study area where LU7 outcrops, whereas the spatial expression of the two highest landslide susceptibility classes decreases in the southwest/south sector were the LU2 outcrops. The ROC curve of the model based on the landslide validation group is shown in Fig. 7. The ROC curve is detached to the upper left corner of ROC space, which confirms the best predictive capacity of the IS susceptibility map when compared with the IV susceptibility map. The AUC of 0.81 also supports the better predictive capacity of the IS model.

As it was already mentioned, shallow landslides in the study area have been triggered by rainfall, typically during intense short duration (1 – 15 days) rainfall events (Zêzere et al., 2005, 2015; Zêzere and Trigo, 2011). Additionally, it is known by extensive field work in the study area (Oliveira, 2012) a total absence of instability signs during the summer, reflecting the dryness that characterizes this season. Therefore, it can be assumed a typical situation of superficial absence of water in the soil during summer, i.e., $m = 0$. Assuming this situation, an additional physically-based shallow slides susceptibility map was prepared considering no water in the soil ($m = 0$). Figure 8B shows the results of modelling. Given the assumed boundary conditions, it was expectable that model do not generate FS $\leq$ 1. However, Fig. 8B shows a small fraction of the study area classified with Very high susceptibility (FS $\leq$ 1, 2.25 % of study area) in a condition of absence of water into the soil, which is interpreted as an error of the IS model. It is worth mentioning that most of the model errors occur over the LU2 (Arranhó formation) indicating that corresponding resistance parameters (cohesion, internal friction angle) may be underestimated.

4.3 Comparison of landslide susceptibility models

The comparison of the susceptibility maps produced with IV and IS methods demonstrates that spatially, the susceptibility ranking differs substantially depending on the method used. Indeed, the Kappa coefficient is only 0.23, which means that spatial correlation is moderate, although the reasonable/good predictive capacity of both models attested by the AUC ROC (Fig.7).

The two highest susceptibility classes in the IV landslide susceptibility map spread over 34.1 % of the total study area and the corresponding percentage of predicted shallow slides approaches 69.4 %. The performance of the predictive model is less interesting for the intermediate susceptibility classes (moderate and low), in particular for the low susceptibility class that includes a relevant portion (15.7 %) of shallow slides belonging to the landslide validation group. The IS landslide susceptibility model reveals a better predictive capacity, which is attested by the presence of 83.1 % of the landslide validation group within the two highest susceptibility classes.

The effective ratios calculated for landslide susceptibility classes of both models are summarized in Table 5. The effective ratios for the IS model are higher for the Very high and High susceptibility classes and lower for the Low and Very low susceptibility classes, which indicate a better predictive capacity when compared with the IV model.

The spatial comparison of the two susceptibility maps is shown in Fig. 9. The value zero means the spatial agreement between landslide susceptibility classes, whereas the other values mean disagreement. Negative values indicate that landslide susceptibility obtained with IV is lower when compared with the map obtained with IS, with the difference increasing from -1 to -4. For example, a grid cell with a score -4 means this terrain unit was classified as very high susceptibility in the IS susceptibility map and as very low susceptibility in the IV susceptibility map. Positive values indicate the opposite relationship between map classes. The perfect spatial agreement between susceptibility classes in both maps occurs in 39.9 % of the study area (Table 6). However, adding the minimum mismatch classification (-1 and +1 in Fig. 9) the previous feature rises to 73 % of the total study area. The major discrepancy between both susceptibility maps (-4, -3, 3 and 4 in Fig. 9) occurs along 10.5 % of the study area, namely where the Abadia formation (LU7) and the Arranhó formation (LU2) outcrop. In the north part of the study area where the LU7 is present, the landslide susceptibility obtained with the IV method is lower when compared with the IS method, whereas the opposite occurs in the central and southern part of the study area where the LU2 is present.

These results can be interpreted according to particular specifications associated with the physically-based and empirically-based methods. The resistance parameters estimated for the superficial soil over LU7 (c '= 2 kPa, φ' = 19 °) are higher than those estimated for LU2 (c '= 0.5 kPa φ '= 17 °). However, the landslide susceptibility computed using the IS tends to be higher over LU7, which is related to the soil water content and eventually to the presence of thicker soils, particularly along the lower part of slopes where topographic conditions are more prone to soil saturation. On the other hand, the empirically-based approach generated IV scores of 0.494 and -0.857, respectively for LU2 and LU7. The positive IV score for LU2 clearly indicates a higher chance for shallow slides occurrence. We admit that shallow slides inventory may be incomplete in the area corresponding to LU7, which could justify the negative IV score. Indeed, the LU7 clays and marls are associated with gentle slopes and are characterized by intense agricultural use; thus, the footprint of small shallow slides is easily erased on the landscape, as the "original" slope profile is recovered for agricultural activities. On the contrary, the LU2 is constituted by sequences of marl and limestone layers, which induce larger topographic irregularities and less productive soils on steep to moderate slopes. These geological and geomorphological conditions favoured along time a land use mainly associated to forest and annual crop cultures. In this context, the landslide footprint over slopes tends to last more in time, which justifies a more complete shallow slides inventory, and consequently, the higher IV score.

4.4. Combination of landslide susceptibility models

The results of the cross-tabulation between landslide susceptibility classes of both susceptibility maps (empirically-based and physically-based) are summarized in a contingency table (Table 6). The distribution of shallow slides belonging to the validation group on the same contingency table is summarized in Table 7. Table 6 also shows the considered combinations within the contingency table to classify the final landslide susceptibility map resulting from the integration of empirically-based and physically-based predictive models, where the colours (red, orange, yellow, light green, green and grey) represent the final susceptibility classes (Very high, High, Moderate, Low, Very low, and uncertain, respectively). The corresponding final shallow slides susceptibility map is shown in Fig. 10 and information about final landslide susceptibility classes is detailed in Table 8.

The Very high susceptibility class covers 16.4 % of the study area and includes 55.6 % of the shallow slides validation group. Similarly, the High susceptibility class covers 14.3 % of the study area and includes 18.6 % of the shallow slides. In opposition, , the Very low and Low susceptibility classes cover 33.4 % and 10.6 % of the study area, respectively, and include only a small fraction of the landslide validation group (1.4 % each class).

Terrain units classified as Very high or High susceptibility by one method and simultaneously as Very low or Low susceptibility by the other method were considered as uncertain regarding susceptibility to shallow slides occurrence in the final map. The 'grey' class, although classified as Uncertain, is potentially High or Very high landslide susceptible and covers 16.3 % of the study area and includes 16.0 % of the shallow slides belonging to the validation group. However, the distribution of landslide validation group in the Uncertain susceptibility class is different in the upper right corner and in the lower left corner of the contingency table (see Tables 6 and 7). Terrain units classified as Very high or High susceptibility by the IS susceptibility map and as Very low or Low susceptibility by the VI method (upper right corner in Tables 6 and 7) includes 14.7 % of shallow slides belonging to the validation group, whereas terrain units with inverse classification (lower left corner in Tables 6 and 7) only contain 1.2 % of the shallow slides validation group. These values, once more, reflect the higher quality of the physically-based susceptibility model in comparison with the empirically-based model.

The predictive quality of susceptibility classes constituting the final landslide susceptibility map is demonstrated by the estimated effective ratios (Table 8). The effective ratio of the Very high susceptibility class (3.39) is higher than those obtained for the equivalent susceptibility class with the empirically-based and physically-based methods (cf. Table 5). In addition, effective ratios corresponding to the Very low and Low susceptibility classes (0.04 and 0.12, respectively) are lower than those obtained with empirically-based and physically-based methods (cf. Table 5), which indicates a better predictive performance. Moreover, the effective ratio is higher for the Uncertain class than for the Moderate class (Table 8), which is consistent with the potential for high or very high susceptibility considered for the Uncertain class.

5 Conclusion

Empirically-based and physically-based methods used to assess landslide susceptibility at the basin scale are conceptually distinct as the former are based on weighting environment predisposing factors, whereas the latter are supported by the computation of shearing and resistance forces along potential slip surfaces. The existence of a landslide inventory is crucial to weight predictive variables within empirically-based methods, which is not the case of physically-based methods that can be computed independently on the landslide inventory. Both types of methods have advantages and drawbacks. The major constrains associated to empirically-based approaches have been summarized in previous works (Corominas et al., 2014; Fell et al., 2008a) and result from: (i) the difficulty of establishing causal (cause-effect) relationships between variables; (ii) problems arising from self-correlation between variables; (iii) the typically not normal statistical distribution of predictor variables; (iv) the limitations related to the quality of data, in particular the completion of the landslide inventory; and (v) the difficulty in transferring the results from the study area to other areas, even with similar characteristics. In the case of physically-based methods, the major constrains were listed as follow (Corominas et al., 2014; Fell et al., 2008a): (i) the high level of generalization and/or simplification regarding the spatial distribution of geotechnical or hydrological parameters; (ii) the feasibility of model application is limited to areas with relatively homogeneous ground conditions (e.g., geology and geomorphology); (iii) the uncertainties about the depth of the soil and of the slip surface; and (iv) the difficulties in predicting groundwater pore pressures and their relationship with rainfall.

In this work we intent to test two hypotheses: (i) although conceptually distinct, empirically-based and physically-based methods generate similar results concerning susceptibility to shallow slide occurrence; and (ii) a reliable landslide susceptibility map can be obtained for a single study area by combining two landslide susceptibility models (empirically-based vs physically-based).

To achieve the proposed objectives the Information Value method and the Infinite Slope method were chosen to build two landslide susceptibility maps. A shallow slides inventory was separated into two independent landslide groups adopting a temporal criterion. The training group was used twofold to define the statistical relationships between landslides and the dataset of variables assumed as landslide predisposing factors by the IV method, and to calibrate the resistance parameters (cohesion and internal friction angle) within the IS method. The landslide validation group was used to independently validate both susceptibility maps.

When analysed independently, both methods generated good predictive results, although the physically-based model revealed to be more effective to spatially predict shallow landslides, which is attested by the AUC ROC and the effective ratio of landslide susceptibility classes. In addition, the application of the Kappa statistics showed that the overall spatial agreement between susceptibility classes of both maps is only moderate (K = 0.23), so the first hypothesis is only partially confirmed. The major differences were registered over two lithological units (LU2 and LU7) and may result from the probable incompleteness of the shallow slides inventory over LU7, as a consequence of human interventions related to agriculture activities.

The final shallow slides susceptibility map produced by combining the results obtained with the empirically-based and physically-based methods through a contingency table proved to be reliable, as it was shown by the effective ratio of the extreme susceptibility classes (Very high, Low and Very low). Thus, the second hypothesis is confirmed. Furthermore, the combination of both methods allowed the identification of areas classified as uncertain regarding landslide susceptibility but with potential to be highly/very highly susceptible to shallow slides occurrence, which is not possible when using a single landslide susceptibility model.

Author contribution

S. C. Oliveira and J. L. Zêzere conceptualized this study and supervised the complete work. S.C. Oliveira performed field work for landslide inventory and prepared the manuscript with contributions from all co-authors. S. Lajas, J. L. Zêzere and S.C. Oliveira performed field work for soil thickness measurement. S. Lajas prepared the cartographical and statistical input data for empirically-based and physically-based susceptibility modelling and validation. R. Melo contributes to the development of the soil thickness model, and to the estimation of geotechnical and hydrological parameters.

Ackonwledgements

This work was supported by the project FORLAND – Hydrogeomorphologic risk in Portugal: driving forces and application for land use planning (PTDC/ATPGEO/1660/2014) funded by Fundação para a Ciência e a Tecnologia, Portugal (FCT). Sérgio Oliveira has a postdoctoral grant (SFRH/BPD/85827/2012) and Raquel Melo has a PhD grant (SFRH/BD/60872/2009) funded by the Portuguese Foundation for Science and Technology (FCT).

References

Aleotti, P. and Chowdhury, R.: Landslide hazard assessment: summary review and new perspectives, Bull. Eng. Geol. Environ., 58(1), 21–44, doi:10.1007/s100640050066, 1999.

Baptista, V.: Estudo das condições geológico-geotécnicas ocorrentes ao longo do sub-lanço Arruda dos Vinhos / Carregado da auto-estrada A10, Lisboa., 2004.

Brenning, A.: Spatial prediction models for landslide hazards: review, comparison and evaluation, Nat. Hazards Earth Syst.

Sci., 5, 853–862, doi:10.5194/nhess-5-853-2005, 2005.

Bui, D. T., Tuan, T. A., Klempe, H., Pradhan, B. and Revhaug, I.: Spatial prediction models for shallow landslide hazards: a comparative assessment of the efficacy of support vector machines, artificial neural networks, kernel logistic regression, and logistic model tree, Landslides, 13(2), 361–378, doi:10.1007/s10346-015-0557-6, 2016.

Carrara, A., Cardinali, M., Detti, R., Guzzetti, F., Pasqui, V. and Reichenbach, P.: GIS techniques and statistical models in evaluating landslide hazard, Earth Surf. Process. Landforms, 16(5), 427–445, 1991.

Carrara, A., Crosta, G. and Frattini, P.: Comparing models of debris-flow susceptibility in the alpine environment, Geomorphology, 94, 353–378, doi:10.1016/j.geomorph.2006.10.033, 2008.

Carrara, a, Guzzetti, F., Cardinali, M. and Reichenbach, P.: Use of GIS Technology in the Prediction and Monitoring of Landslide Hazard, Nat. Hazards, 20, 117–135, doi:10.1023/A:1008097111310, 1999.

Cascini, L.: Applicability of landslide susceptibility and hazard zoning at different scales, Eng. Geol., 102(3–4), 164–177, doi:10.1016/j.enggeo.2008.03.016, 2008.

Catani, F., Segoni, S. and Falorni, G.: An empirical geomorphology based approach to the spatial prediction of soil thickness at catchment scale, Water Resorces Res., 46, 1–15, doi:10.1029/2008WR007450, 2010.

Cernica, J. N.: Geotechnical Engineering: Soil Mechanics, John Wiley & Sons, New York., 1995.

Cervi, F., Berti, M., Borgatti, L., Ronchetti, F., Manenti, F. and Corsini, A.: Comparing predictive capability of statistical and deterministic methods for landslide susceptibility mapping: A case study in the northern Apennines (Reggio Emilia Province, Italy), Landslides, 7(4), 433–444, doi:10.1007/s10346-010-0207-y, 2010.

Chang, K. and Chiang, S.: An integrated model for predicting rainfall-induced landslides, Geomorphology, 105(3–4), 366–373, doi:10.1016/j.geomorph.2008.10.012, 2009.

Chung, C.-J. F. and Fabbri, A. G.: Validation of Spatial Prediction Models for Landslide Hazard Mapping, Nat. Hazards, 65, 451–472, 2003.

Corominas, J., Westen, C. Van, Frattini, P., Cascini, L., Malet, J.-P., Fotopoulou, S., Catani, F., Eeckhaut, M. Van Den, Mavrouli, O., Agliardi, F., Pitilakis, K., Winter, M. G., Pastor, M., Ferlisi, S., Tofani, V., Herva, J. and Smith, J. T.: Recommendations for the quantitative analysis of landslide risk, Bull. Eng. Geol. Environ., 73, 209–263, doi:10.1007/s10064-013-0538-8, 2014.

Crosta, G., Carrara, A., Agliardi, F., Campedel, P. and Frattini, P.: Valutazione della pericolosità da caduta massi tramite un approccio integrato statistico e deterministico, G. di Geol. Appl., 4, 41–48, 2006.

Cruden, D. and Varnes, D.: Landslides types and processes, in Landslides investigation and mitigation, edited by A. Turner and R. Schuster, pp. 36–75, Transportation Research Board. National Academic Press, Washington DC., 1996.

Davis, J. C., Chung, C. J. and Ohlmacher, G. C.: Two models for evaluating landslide hazards, Comput. Geosci., 32(8), 1120–1127, doi:10.1016/j.cageo.2006.02.006, 2006.

Dietrich, W. and Montegomery, D.: SHALSTAB: A digital terrain model for mapping shallow landslide potential., 1998.

Felicísimo, Á., Cuartero, A., Remondo, J. and Quirós, E.: Mapping landslide susceptibility with logistic regression, multiple adaptive regression splines, classification and regression trees, and maximum entropy methods: A comparative study, Landslides, 10(2), 175–189, doi:10.1007/s10346-012-0320-1, 2013.

Fell, R., Corominas, J., Bonnard, C., Cascini, L., Leroi, E. and Savage, W. Z.: Commentary. Guidelines for landslide susceptibility, hazard and risk zoning for land-use planning, Eng. Geol., 102(3–4), 99–111, doi:10.1016/j.enggeo.2008.03.014, 2008a.

Fell, R., Corominas, J., Bonnard, C., Cascini, L., Leroi, E. and Savage, W. Z.: Guidelines for landslide susceptibility, hazard and risk zoning for land use planning, Eng. Geol., 102(3–4), 85–98, doi:10.1016/j.enggeo.2008.03.022, 2008b.

Fernandes, M. M.: Mecânica dos solos. Volume I, FEUP, Porto., 1994.

Ferreira, A.: Mouvements de terrain dans la region au nord de lisbonne. Condition morphostructurales et climatiques, in Mouvements de terrain, pp. 485–494, Paris., 1984.

Ferreira, A., Zêzere, J. and Rodrigues, M.: Instabilite des versants dans la region au nord de Lisbonne. Essai de cartographie geomorphologique, Finisterra, XXII(44), 227–246, 1987.

Fonseca, I.: Modelling soil properties at the landscape scale in a desertification context, King's College London., 2005.

Formetta, G., Rago, V., Capparelli, G., Rigon, R., Muto, F. and Versace, P.: Integrated Physically based system for modeling landslide susceptibility, Procedia Earth Planet. Sci., 9, 74–82, doi:10.1016/j.proeps.2014.06.006, 2014.

Frattini, P., Crosta, G., Carrara, A. and Agliardi, F.: Assessment of rockfall susceptibility by integrating statistical and physically-based approaches, Geomorphology, 94, 419–437, doi:10.1016/j.geomorph.2006.10.037, 2008.

Geotechdata: Angle friction, http://geotechdata.info/parameter/angle-of-friction.html (as of September 14.12.2013), 2013.

Goetz, J. N., Guthrie, R. H. and Brenning, A.: Geomorphology Integrating physical and empirical landslide susceptibility models using generalized additive models, Geomorphology, 129, 376–386, doi:10.1016/j.geomorph.2011.03.001, 2011.

Gorsevski, P. V., Gessler, P. E. and Jankowski, P.: Integrating a fuzzy k-means classification and a Bayesian approach for spatial prediction of landslide hazard, J. Geogr. Syst., 5(3), 223–251, doi:10.1007/s10109-003-0113-0, 2003.

Guillard, C. and Zêzere, J.: Landslide Susceptibility Assessment and Validation in the Framework of Municipal Planning in Portugal : The Case of Loures Municipality, Environ. Manage., 50, 721–735, doi:10.1007/s00267-012-9921-7, 2012.

Guzzetti, F.: Landslide hazard and risk assessment, Rheinischen Friedrich-Wilhelms, Universität Bonn., 2005.

Guzzetti, F., Carrara, A., Cardinali, M. and Reichenbach, P.: Landslide hazard evaluation: A review of current techniques and their application in a multi-scale study, Central Italy, Geomorphology, 31(1–4), 181–216, doi:10.1016/S0169-555X(99)00078-1, 1999.

Hutchinson, J.: Keynote paper: Landslide hazard assessment, in Landslides, edited by D. Bell, pp. 1805–1841, Balkema, A.A., Rotterdam., 1995.

INETI: Carta geológica da Área Metropolitana de Lisboa na escala 1:25000., 2005.

Jenness, J., Brost, B. and Beier, P.: Land Facet Corridor Designer: Extension for ArcGIS, 2011.

Jeremias, F. T.: Geological Controls on the Engineering Properties of Mudrocks of the North Lisbon Area, Tese de Doutoramento, Department of Civil and Structural Engineering, University of Sheffield., 2000.

Lee, S., Ryu, J.-H. and Kim, I.-S.: Landslide susceptibility analysis and its verification using likelihood ratio, logistic regression, and artificial neural network models: case study of Youngin, Korea, Landslides, 4(August 2006), 327–338, doi:10.1007/s10346-007-0088-x, 2007.

Lencastre, A. and Franco, F.: Lições de hidrologia, Fundação para a Ciência e a Tecnologia, Lisboa., 2006.

Montgomery, D., Sullivan, K. and Greenberg, H.: Regional test of a model for shallow landsliding, Hydrol. Process., 12, 943–945, 1998.

O' Loughlin, E.: Prediction of surface saturation zones in natural catchments by topographic analysis, Water Resour. Res., 22(5), 794–804, 1986.

O'Callagham, J. and Mark, D.: The extraction of drainage networks from digital elevation data, Comput. Vision, Graph. Image Process., 28(3), 323–344, 1984.

Oliveira, S. C.: Incidência espacial e temporal da instabildiade gemorfológica na bacia do rio Grande da Pipa (Arruda dos Vinhos), Instituto de Geografia e Ordenamento do Território. Universidade de Lisboa., 2012.

Oliveira, S. C., Zêzere, J. L., Catalão, J. and Nico, G.: The contribution of PSInSAR interferometry to landslide hazard in weak rock-dominated areas, Landslides, 12(4), 703–719, doi:10.1007/s10346-014-0522-9, 2015.

Piacentini, D., Devoto, S., Montovani, M., Pasuto, A., Prampolini, M. and Soldati, M.: Landslide susceptibility modeling assisted by Persistent Scatterers Interferometry (PSI): an example from the northwestern coast of Malta, Nat. Hazards, 78, 681–697, doi:10.1007/s11069-015-1740-8, 2015.

Pimenta, R.: Avaliação da susceptibilidade à ocorrência de movimentos de vertente com métodos de base física, Faculdade de Ciências, Universidade de Lisboa., 2011.

Pradham, A. and Kim, Y.-T.: Application and comparison of shallow landslide susceptibility models in weathered granite soil under extreme rainfall events, Environ. Earth Sci., 73, 5761–5771, doi:10.1007/s12665-014-3829-x, 2015.

Rawls, W., Brakensiek, D. and Saxton, K.: Estimation of soil water properties, Trans. ASAE, 25(5), 1316–1320 and 1328, 1982.

Sawatzky, D. L., Raines, G. L., Bonham-Carter, G. F. and Looney, C. G.: ArcSDM: ArcMAP extension for spatial data modelling using weights of evidence, logistic regression, fuzzy logic and neural network analysis., 2008.

Sharma, S.: Slope stability concepts, in Slope stability and stabilization methods, edited by L. W. Abramson, T. S. Lee, and G. M. Sharma, S E, Boyce, pp. 329–461, John Wiley & Sons Inc., New York., 2002.

Sørensen, R., Zinko, U. and Seibert, J.: On the calculation of the topographic wetness index : evaluation of different methods based on field observations, Hydrol. Earth Syst. Sci., 10, 101–112, 2006.

Süzen, M. and Doyuran, V.: A comparison of the GIS based landslide susceptibility assessment methods : multivariate versus bivariate, Environ. Geol., 45, 665–679, doi:10.1007/s00254-003-0917-8, 2004.

Teixeira, M., Bateira, C., Marques, F. and Vieira, B.: Physically based shallow translational landslide susceptibility analysis in Tibo catchment , NW of Portugal, Landslides, 12, 455–468, doi:10.1007/s10346-014-0494-9, 2015.

Trigo, R. M., Zêzere, J. L., Rodrigues, M. L. and Trigo, I. F.: The Influence of the North Atlantic Oscillation on Rainfall

Triggering of Landslides near Lisbon, Nat. Hazards, 36, 331–354, doi:10.1007/s11069-005-1709-0, 2005.

Vallejo, L., Ferrer, M., Ortuño, L. and Oteo, C.: Ingeniería Geológica., Pearson Educación, Madrid., 2002.

Varnes, D., Slopes, I. A. of E. G. and On, C. on L. and O. M. M.: Landslide hazard zonation: a review of principles and practice, edited by Unesco, Paris., 1984.

Visser, H. and Nijs, T.: The Map Comparison Kit, Environ. Model. Softw., 21, 346–358, 2006.

Yilmaz, I. and Keskin, I.: GIS based statistical and physical approaches to landslide susceptibility mapping (Sebinkarahisar , Turkey), Bull. Eng. Geol. Environ., 68, 459–471, doi:10.1007/s10064-009-0188-z, 2009.

Yin, K. L. and Yan, T. Z.: Statistical prediction models for slope instability of metamorphic rocks, in Landslides, edited by C. Bonnard, pp. 1269–1272, Balkema, Rotterdam., 1988.

Zbyszewski, G. and Assunção, C. T.: Notícia explicativa da folha 30-D (Alenquer). Carta Geológica de Portugal., Serviços Geológicos de Portugal, Lisboa., 1965.

Zêzere, J. L.: As costeiras a Norte de Lisboa: Evolução quaternária e dinâmica actual das vertentes, Finisterra, XXVI(51), 27–56, 1991.

Zêzere, J. L.: Landslide susceptibility assessment considering landslide typology . A case study in the area north of Lisbon (Portugal), Nat. Hazards Earth Syst. Sci., 2, 73–82, 2002.

Zêzere, J. L. and Rodrigues, M. L.: Rainfall Thresholds for Landsliding in Lisbon Area (Portugal), in Landslides, edited by J. Rybar, J. Stemberk, and P. Wagner, A.A. Balkema Publishers, Lisse., 2002.

Zêzere, J. L. and Trigo, R. M.: Impacts of the North Atlantic Oscillation on Landslides, in Hydrologicall, Socioeconomic and ecological impacts of the North Atlantic Oscillation in the Mediterranean Region, edited by S. Vicente-Serrano and R. Trigo, pp. 199–212, Springer., 2011.

Zêzere, J. L., Ferreira, A. B. and Rodrigues, M. L.: Landslides in the North of Lisbon Region (Portugal): Conditioning and Triggering Factors, Phys. Chem. Earth, 24(10), 925–934, 1999.

Zêzere, J. L., Trigo, R. M. and Trigo, I. F.: Shallow and deep landslides induced by rainfall in the Lisbon region (Portugal): assessment of relationships with the North Atlantic Oscillation, Nat. Hazards Earth Syst. Sci., 5, 331–344, 2005.

Zêzere, J. L., Vaz, T., Pereira, S., Oliveira, S. C., Marques, R. and Garcia, R. A. C.: Rainfall thresholds for landslide activity in Portugal: a state of the art, Environ. Earth Sci., 73(6), 2917–2936, doi:10.1007/s12665-014-3672-0, 2015.

Zizioli, D., Meisina, C., Valentino, R. and Montrasio, L.: Comparison between different approaches to modeling shallow Atmospheric landslide susceptibility : a case history in Oltrepo Pavese , Measurement Northern Italy, Nat. Hazards Earth Syst. Sci., 13, 559–573, doi:10.5194/nhess-13-559-2013, 2013.

Table 1. Shallow slides inventory characteristics

Study area (km²)	Training group		Validation group		Total inventory	
	# slides	area (km²)	# slides	area (km²)	# slides	area (km²)
13.9	51	0.027	60	0.030	111	0.057

Table 2. K_c constant calibration parameter for each lithological unit

LU	Description	# Field soil measurement points	K_c
1	Alluvium	0	2.9
2	Arranhó formation: limestone and marls	57	1.5
3	Sobral formation: sandstones and limestones	0	3.6
4	Sobral formation: clays and marls	16	3.6
5	Amaral formation: limestones	15	2.3
6	Amaral formation : marls	1	2.9
7	Abadia formation: clays and marls	21	4.3
8	Dykes and volcanic mass	0	2.9

Table 3. Geotechnical parameters assign to each lithological unit

LU	Specific soil weigh (mean values)t			Cohesion	Internal friction angle
	Saturated soil (kN/m^3)	Natural soil (kN/m^3)	Submerged soil (kN/m^3)	(kPa)	(°)
1	17.5	16.5	7.69	3	19
2	20.9	19.9	11.1	0.5	17
3	20.6	19.6	10.8	2	16
4	20.6	19.6	10.8	2	15
5	20.9	19.9	11.1	1.5	24
6	19.6	18.6	9.8	3	19
7	19.6	18.6	9.8	2	19
8	26	25	16.2	50	35

Table 4. Information Value scores for each class of landslide predisposing factor.

Predisposing factor	ID	Description	# Pixels	# Pixels with landslides	IV
Lithology	1	Alluvium	2064	0	-1,760
	2	Arranhó formation: limestone and marls	217575	17525	0,494
	3	Sobral formation: sandstones and limestones	3771	500	0,993
	4	Sobral formation: clays and marls	95106	3775	-0,213
	5	Amaral formation: limestones	92363	2400	-0,637
	6	Amaral formation : marls	4331	175	-0,196
	7	Abadia formation: clays and marls	131898	2750	-0,857
	8	Dykes and volcanic mass	5911	50	-1,759
Land Use	1	Pinus pinaster forest	1803	0	-2,187
	2	Eucalyptus forest	9874	0	-2,187
	3	Mixed forest	39044	2500	0,265
	4	Broadleaf forest	1198	0	-2,187
	5	Poor natural pasturages	223	0	-2,187
	6	Sclerophytic vegetation	9096	0	-2,187
	7	Low shrubs	27172	150	-2,186
	8	High shrubs and degraded or transition forest	2792	725	1,665
	9	Forest and annual agricultural areas	114403	6000	0,065
	10	Orchard and annual agricultural areas	5334	0	-2,187
	11	Orchard and vineyards	3014	0	-2,187
	12	Mixed cultures and orchard	765	0	-2,187
	13	Annual agricultural areas and forest	13889	425	-0,474
	14	Annual agricultural areas and vineyards	104697	3600	-0,357
	15	Olive grove	279	0	-2,187
	16	Olive grove and orchard	3	0	-2,187
	17	Vineyards	56424	10000	1,283
	18	Vineyards and orchard	39126	750	-0,941
	19	Vineyards and olive grove	844	0	-2,187
	20	Complex cultural systems	104453	3025	-0,529
	21	Continuous urban areas	521	0	-2,187
	22	Discontinuous urban areas	14954	0	-2,187
	23	Industrial and commercial areas	930	0	-2,187
	24	Other urban infrastructures	1268	0	-2,187

	25	Degraded areas	489	0	-2,187
	26	Other spaces outside the consolidated urban areas	424	0	-2,187
Slope (º)	1	0 – 5	71241	375	-2,234
	2	5 – 10	207252	4675	-0,779
	3	10 – 15	156344	9525	0,215
	4	15 – 20	67852	3925	0,163
	5	20 – 25	27892	3600	0,966
	6	25 – 30	12284	1850	1,120
	7	30 – 35	5770	1800	1,848
	8	>35	4384	1425	1,889
Aspect	1	Flat	986	0	-0,886
	2	North	82435	3450	-0,161
	3	Northeast	66693	8725	0,979
	4	East	99656	5350	0,088
	5	Southeast	69065	1400	-0,885
	6	South	33558	0	-0,886
	7	Southwest	55920	1875	-0,382
	8	West	72192	2350	-0,412
	9	Northwest	72514	4025	0,122
Profile slope curvature	1	Convex (0,05 – 1,47)	190076	7525	-0,216
	2	Straight/Flat (-0,05 – 0,05)	128858	4025	-0,453
	3	Concave (0,05 – 1,22)	234085	15625	0,306
Topographic Position Index (TPI)	1	-21,23 – -12,49	5718	750	0,982
	2	-12,49 – -7,53	30746	4800	1,156
	3	-7,53 – -2,57	130188	9350	0,379
	4	-2,57 – 2,39	210933	6300	-0,498
	5	2,39 – 7,35	115609	4175	-0,308
	6	7,35 – 31,83	59825	1800	-0,491
Slope Over Area Ratio (SOAR)	1	0	5052	250	0,007
	2	0 – 0,00001	2261	300	0,993
	3	0,00001 – 0,0001	4241	50	-1,427
	4	0,0001 – 0,001	17928	750	-0,161
	5	0,001 – 0,01	167668	6000	-0,317
	6	0,01 – 0,1	298168	14750	0,007
	7	> 0,1	57701	5075	0,582

Table 5. Effective ratio of classes defined for the IV and IS shallow slide susceptibility maps

	IV method			IS method		
Susceptibility class	Class area (%)	Landslide validation group area (%)	Effective ratio	Class area (%)	Landslide validation group area (%)	Effective ratio
Very high	18.00	48.98	2.72	17.93	53.35	2.98
High	16.15	20.39	1.26	16.05	29.72	1.85
Moderate	14.02	11.74	0.84	14.06	11.66	0.83
Low	18.88	15.65	0.83	18.97	3.76	0.20
Very low	32.94	3.64	0.10	32.99	1.50	0.05

Table 6. Contingence table extracted from the overlay of IV and IS shallow slide susceptibility maps in % of the study area. Colours represent the susceptibility classes of the final map: Red – Very high; Orange – High; Yellow – Moderate; Light green – Low; Green – Very low; Grey – Uncertain, but with potential for high/very high susceptibility.

ISM map\IV map	Very high	High	Moderate	Low	Very low	Total
Very high	8.0	3.9	2.2	2.0	1.1	17.3
High	4.5	3.9	3.0	2.9	1.8	16.1
Moderate	2.3	2.9	2.7	3.3	3.0	14.2
Low	2.1	2.9	3.1	4.6	6.5	19.2
Very low	1.2	2.2	3.0	6.2	20.7	33.3
Total	18.0	15.8	14.0	19.0	33.2	100

Table 7. Distribution (%) of shallow slides of the validation group in classes obtained by overlay IV and IS shallow slide susceptibility maps.

ISM map\IV map	Very high	High	Moderate	Low	Very low	Total
Very high	24.8	12.0	3.6	9.1	2.6	52.1
High	18.8	5.7	2.5	2.6	0.4	30.0
Moderate	4.5	2.3	3.9	1.7	0.2	12.5
Low	0.9	0.3	1.7	1.0	0.0	3.8
Very low	0.0	0.0	0.2	1.3	0.1	1.5
Total	49.0	20.3	11.8	15.7	3.2	100

Table 8. Susceptibility classes and correspondent effective ratios of the final shallow slides susceptibility map

Susceptibility class	# Pixels	Unstable area (m2)	Study area %	Unstable area %	Effective ratio
Very high	90786	18475	16.4	55.6	3.39
High	78678	6175	14.2	18.6	1.31
Moderate	50560	2400	9.1	7.2	0.79
Low	58456	425	10.6	1.3	0.12
Very low	184528	450	33.4	1.4	0.04
Uncertain – with potential to high or very high	90011	5300	16.3	16.0	0.98
Total	553019	33225	100	100	--

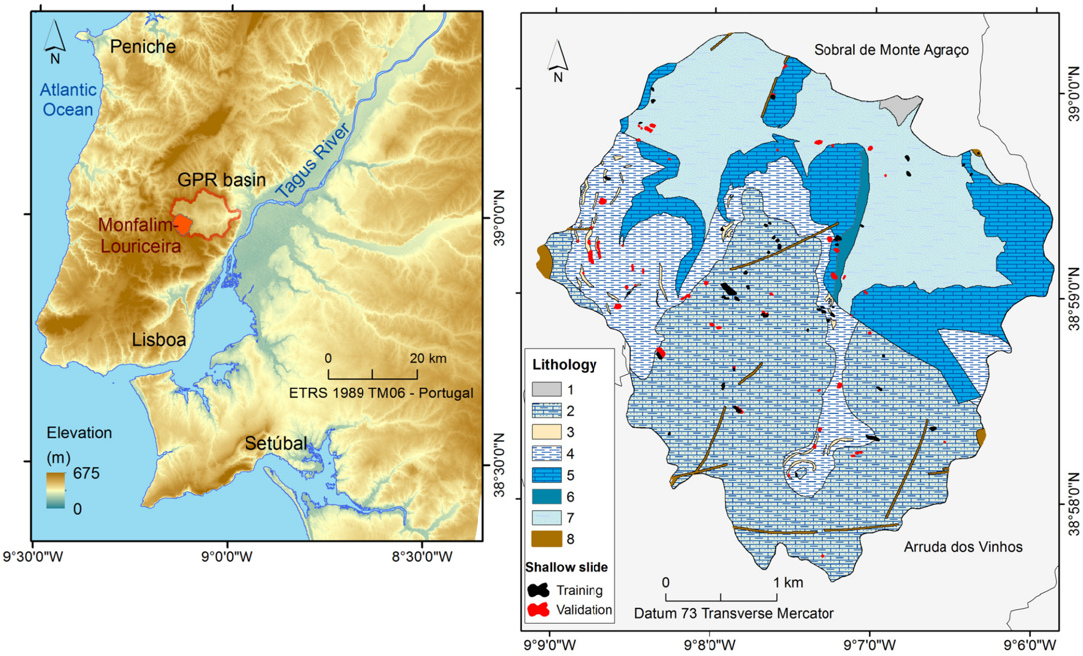

Figure 1: Location of Monfalim – Louriceira study area and spatial distribution of lithological units.

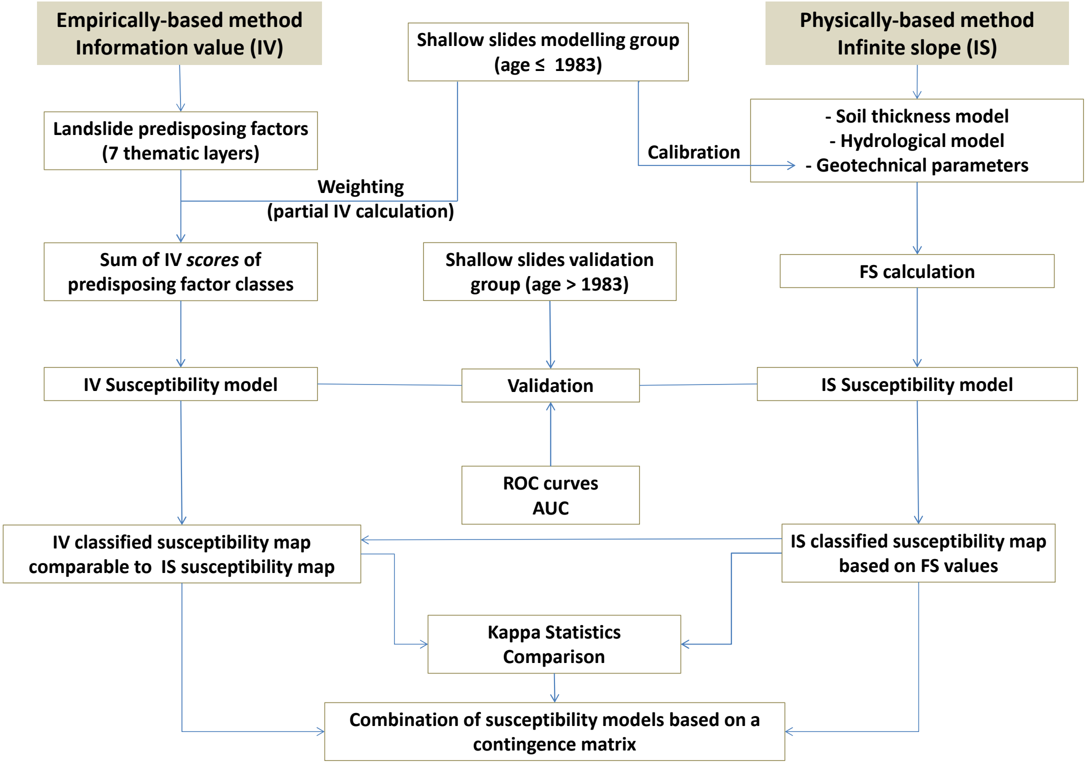

Figure 2: Methodological framework to compare and to combine empirically-based and physically-based landslide susceptibility models.

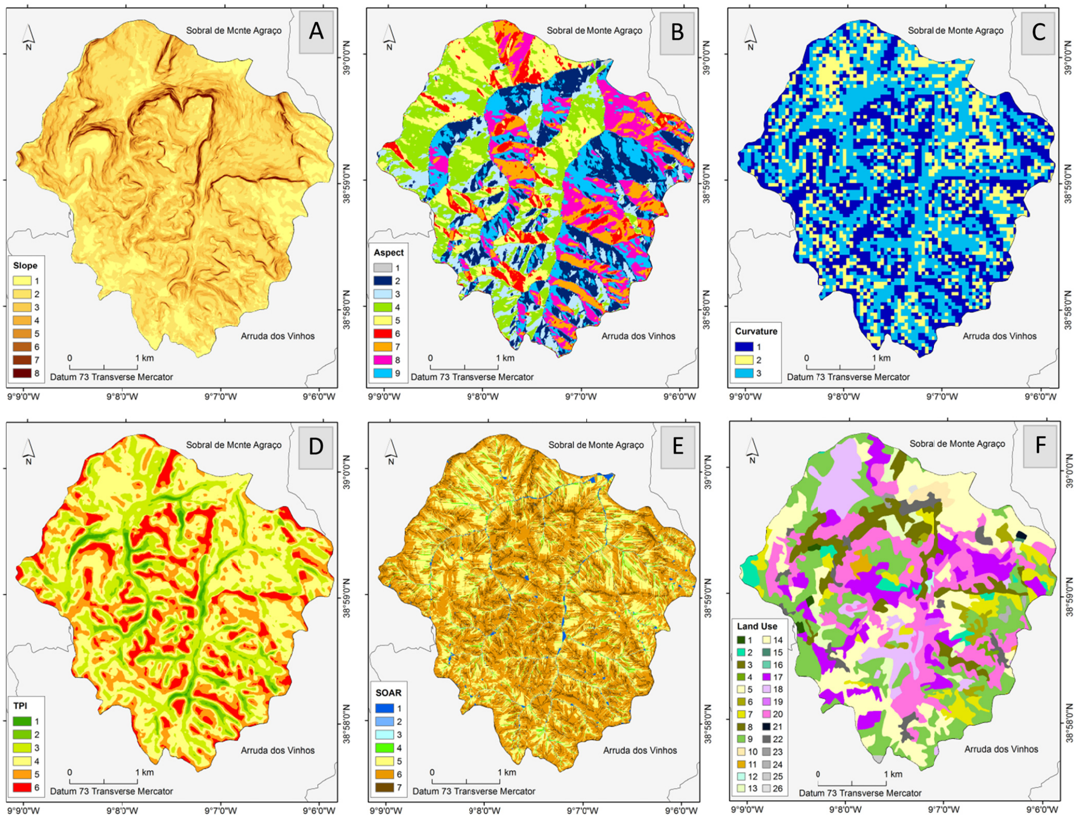

5

Figure 3: Dataset of shallow slides predisposing factors. Lithology is shown in Figure 1.

10

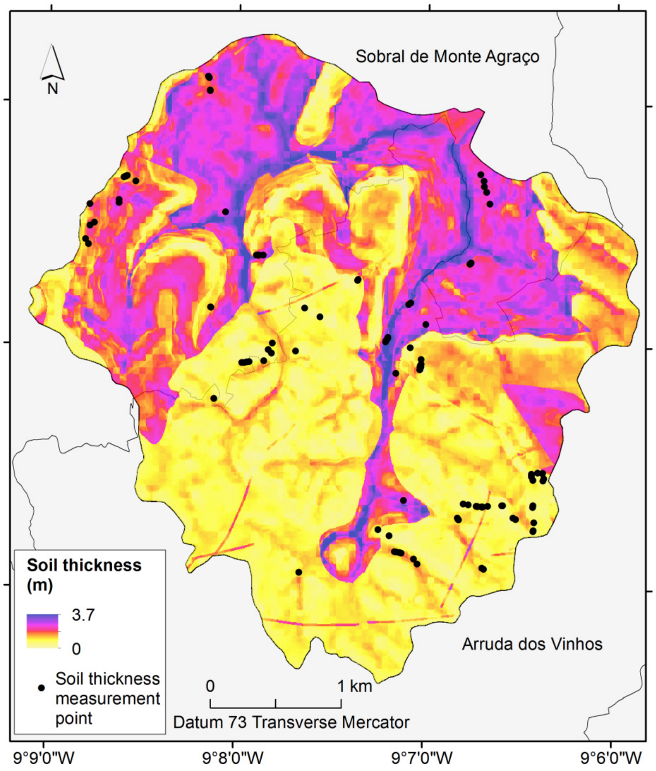

5

Figure 4: Soil depth map.

10

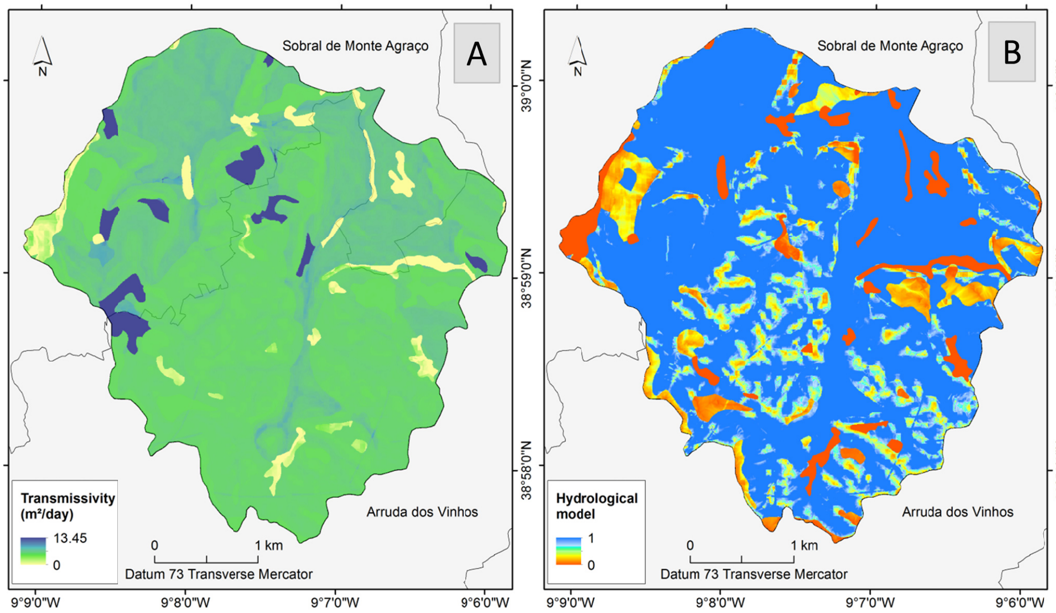

Figure 5: Transmissivity (A) and hydrological model (B) of the study area.

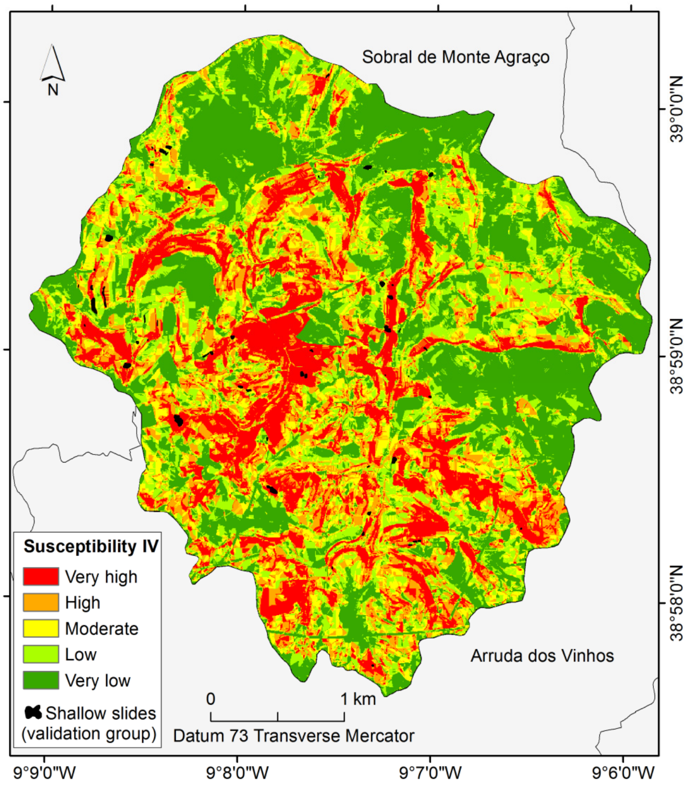

Figure 6: IV Shallow slides susceptibility map.

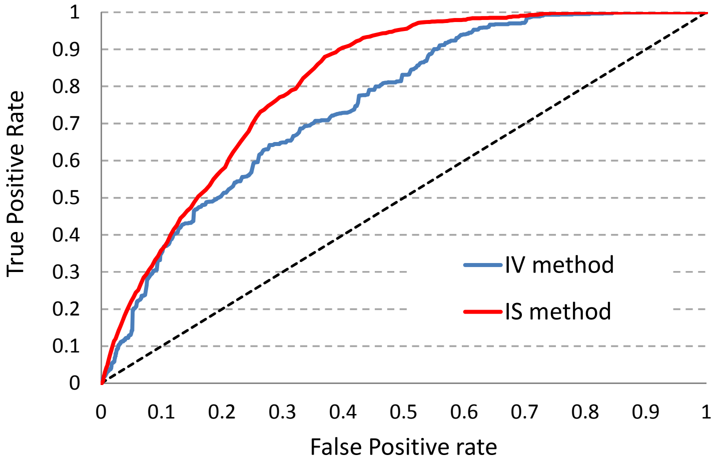

Figure 7: ROC curves based on independent validation of IV and IS shallow slides susceptibility models.

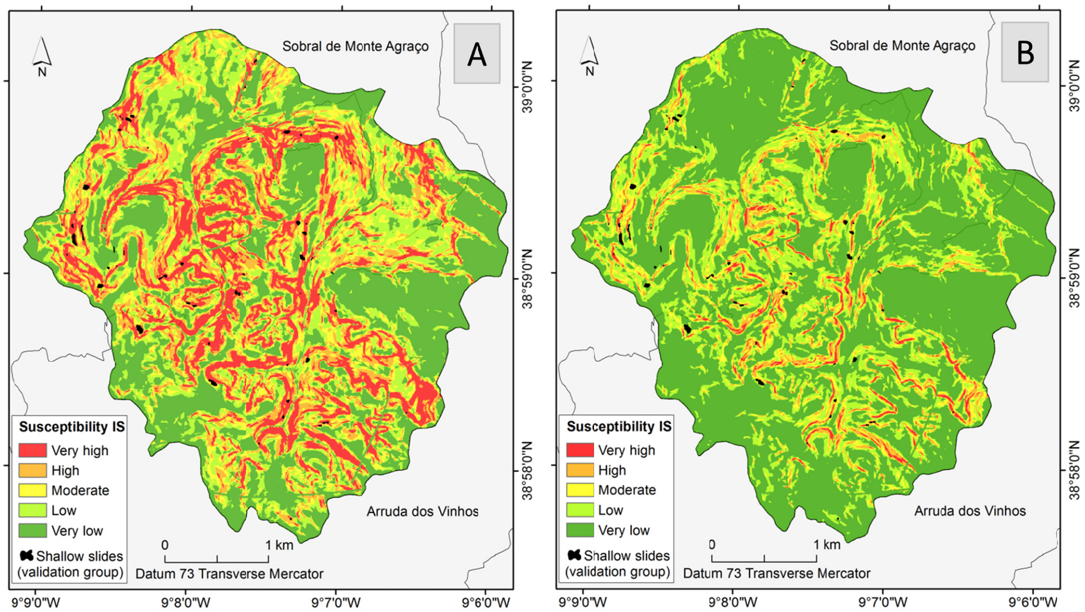

Figure 8: IS shallow slides susceptibility maps (A) m according to figure 5b; (B) m = 0.

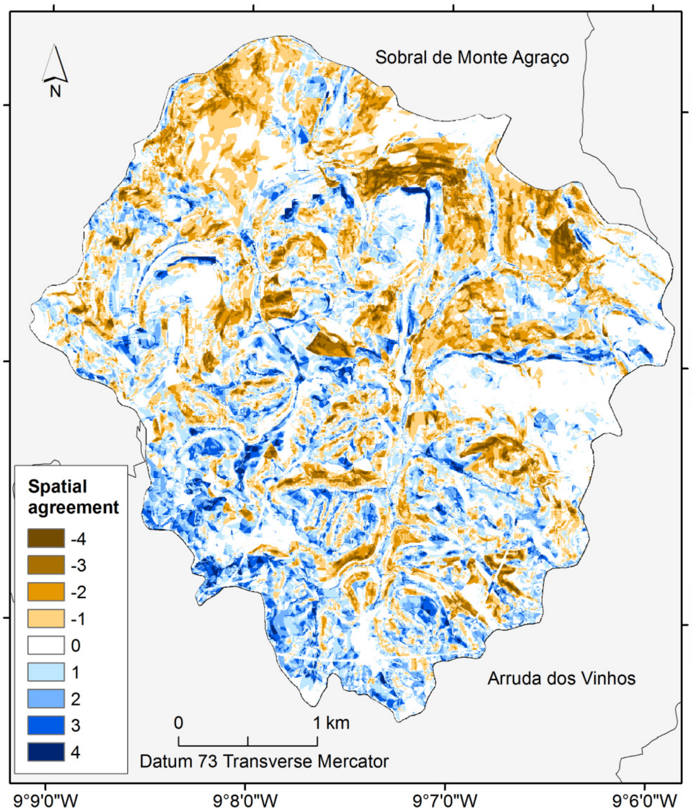

5

Figure 9: Spatial agreement between IV and IS shallow slides susceptibility maps. 0 means full agreement; 4 and -4 means maximum disagreement.

10

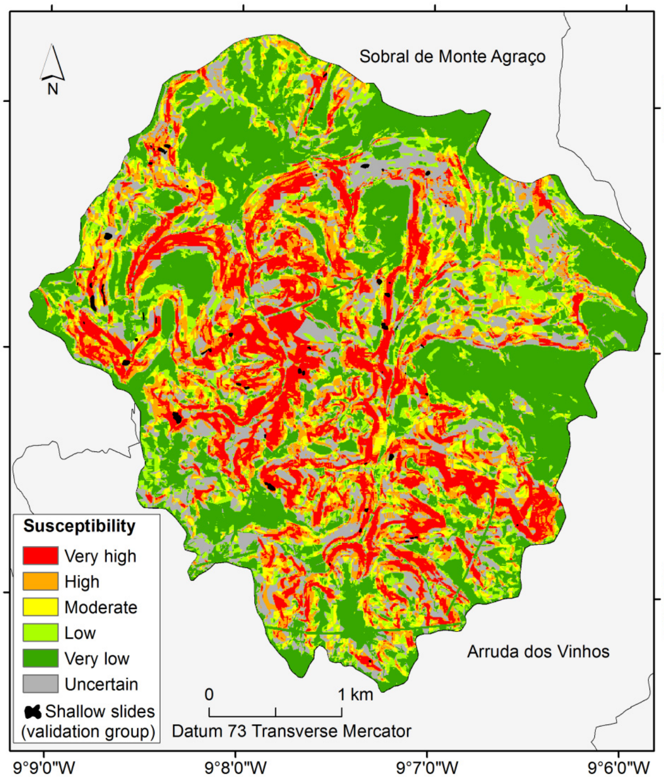

5

Figure 10: Final shallow slides susceptibility map resulting from the combination of IV and IS susceptibility maps.

10